Processing and Application of Ceramics 14 [1] (2020) 40–46
https://doi.org/10.2298/PAC2001040B

Synthesis and characterization of hydrophobic nano-silica thin coatings for outdoor insulators

Khashayar Beirami[1], Saeid Baghshahi[2,*], Mohammad Ardestani[1], Nastaran Riahi[3]

[1]*Department of Materials Engineering, Science and Research Branch, Islamic Azad University, Tehran, Iran*
[2]*Department of Materials Science and Engineering, Faculty of Engineering, Imam Khomeini International University, Qazvin, Iran*
[3]*Non-Metalic Materials Research Group, Niroo Research Institute (NRI), Tehran, Iran*

Received 10 June 2019; Received in revised form 29 November 2019; Accepted 3 February 2020

Abstract

The hydrophobic characteristics of outdoor insulator surface have significant influence on the lifetime and performance of the power transmission lines. In this research, a textured silica layer was dip-coated on the surface using a tetraethyl-orthosilicate (TEOS) containing solution in order to create a hydrophobic surface. Subsequently, the created coating was modified by dipping it in an octadecyl-trichloro-silane/ethanol solution to decrease its surface energy. The coating was characterized by field emission scanning electron microscopy, X-ray diffraction method, Fourier-transform infrared spectroscopy and atomic force microscopy. The microstructural studies confirmed the formation of a uniform microstructure with the mean particle size of 19 nm and roughness of less than 80 nm. The results demonstrated that by creating the hydrophobic coating, the contact angle increased from 14 to 120°. The result of leakage current test at 10 kV showed that the leakage current of the coated insulator was about 24.4 μA, while that of the non-coated one was about 32 μA. The adhesion strength of the coating was 1.7 MPa.

Keywords: *outdoor insulators, silica coating, hydrophobic, contact angle, leakage current*

I. Introduction

Coating is one of the effective methods to modify the properties of the surface. By preparing a uniform coating with controlled particle size, a surface with desired properties could be achieved. Nowadays, the nanostructured ceramic coatings are widely used in different industrial fields. The nanostructured ceramic coatings improve the hydrophobic and self-cleaning properties of the outdoor insulators [1–4]. In different climate regions and especially in the ones with a relatively high level of pollution, the presence of particle contaminations has a negative effect on the performance of the outdoor insulators. Creating the nanostructured coatings on the surface of outdoor insulators enhances the performance of these devices by fixing the flashover phenomena, which is one of the main problems in the polluted wet areas. Moreover, the weak adhesion of the conventional coatings to the substrate is not observed in the nanostructured coating, which is the result of the small particle size of this group of coatings. There are various methods for the preparation of nanostructured coatings, including PVD, CVD, sol-gel and co-precipitation [5]. The methods which involve high pressures and temperatures are always encountered with different technical problems, such as the phase transformations of the substrate during densification of the coating and also thermal expansion mismatch of the coating and the substrate [6]. However, the processing temperature in the sol-gel method is relatively low and the synthesized coatings made by this method are uniform. Sol-gel has been used for synthesizing the crystalline and amorphous coatings. Super hydrophobic surfaces can be obtained either by creating a rough surface with low surface energy or by modifying a rough surface by a material with low surface energy.

Silica is one of the most important materials for making hydrophobic and self-cleaning coatings [7–9]. Ramala *et al.* [10] applied silica coatings on porcelain insulators. They reported that the contact angle of the coatings was higher than 150° and had desirable adhesion

*Corresponding author: tel: +98 912 2164225,
e-mail: *baghshahi@eng.ikiu.ac.ir*

to the substrate. Pantoja *et al.* [11] investigated the effect of the type of solvent on the hydrophobic properties of silica and silane containing coatings. They showed that the type of solvent has a significant effect on the hydrophobic properties of the coating. The highest angle which they reported was 90°. In another investigation, Dou *et al.* [12] investigated the photonic properties of silica coating on the antireflective glass. They used perfluoro-decyl-trichoxy silane for decreasing the surface energy of the coating. They reported a contact angle of 136°.

One of the shortcomings which restrict the application of silica coatings is the weak adhesion of the coating to the substrate and also low hydrophobic property due to the deposition of dust on the coating in workplace. It has been found that by decreasing the coating particle size, the adhesion of the particles to the substrate increased [12]. Therefore, making the coatings with small particle size leads to better adhesion and increases the useful operating time. In this research, hydrophobic nanosized coatings with small particle size were applied on glass substrates and also glazed outdoor insulators via sol-gel method. In the applied method, at first the substrate was coated by SiO_2 nanoparticles and then by a material with low surface energy (using octadecyl-trichloro-silane solution) in order to modify the rough surface.

II. Experimental

High purity tetraethyl-orthosilicate (TEOS), octadecyl-trichloro-silane (OTS), ethanol and HCl were supplied by Merck. The coating was first prepared on a glass substrate to determine the optimum conditions and then on the insulator. At the first stage, in order to create the coating, three TEOS and water solutions with predetermined molar ratios were prepared according to Table 1. Then HCl with concentration of 7.9×10^{-4} mol/l was added to the prepared solutions and the pH was adjusted to 3. The prepared solution was stirred via magnetic stirrer at 75 °C for 2 h. Subsequently, the solution was stirred by magnetic stirrer with the rate of 150 rpm at room temperature for 24 h.

Table 1. Molar ratios of precursors in the prepared solutions

Sample	Distilled water	Ethanol	TEOS
S1	13	15	1
S2	13	22	1
S3	13	30	1

To coat the glass substrates, the samples were immersed (dip-coated) in the prepared solutions with the rate of 1 mm/s by an immersion coating apparatus for 10 min. The coated samples were dried at 70 °C for 15 min followed by heat treatment at 200 °C. The coating which was prepared from the S2 solution was additionally dipped in the solutions containing 2, 5 and 7 vol.% of OTS in ethanol for 10 s. Then the specimens were dried at 120 °C for 2 h. Finally, based on the obtained results, the insulators were dip-coated with the S2 solution.

The prepared coatings were characterized by X-ray diffraction (XRD) using a Philips X-ray diffractometer with Cu Kα radiation (λ = 1.540598 Å) within the 2θ angle range from 10 to 80°. The morphology and microstructure of the coatings were investigated by Hitachi S4160 field emission scanning electron microscope (FESEM) equipped by energy dispersive spectroscopy (EDS) analyser. Atomic force microscope (AFM, Veeco/CP-Research) was used to evaluate the roughness of the coatings. Fourier transform infrared spectroscopy (FTIR, JASCO-410) was used to obtain the infrared absorption spectrum of the coatings in the range of 400–4000 cm^{-1}. The thermogravimetric analysis of the coatings was examined up to 1000 °C with a heating rate of 10 °C/min in nitrogen atmosphere. The adhesion strength of the coating to the substrate was determined according to ASTM D 4541 standard. The contact angle was measured via protractor (OCA115/PLUS) equipped with a CCD camera. The leakage current of the coated and uncoated insulator was measured in an atmosphere with 80% humidity at 2.9 to 10 kV ranges.

III. Results and discussion

3.1. Characterization of the prepared SiO_2 coatings

Figure 1 shows the FESEM micrograph of the surface of different coatings before modification by the OTS so-

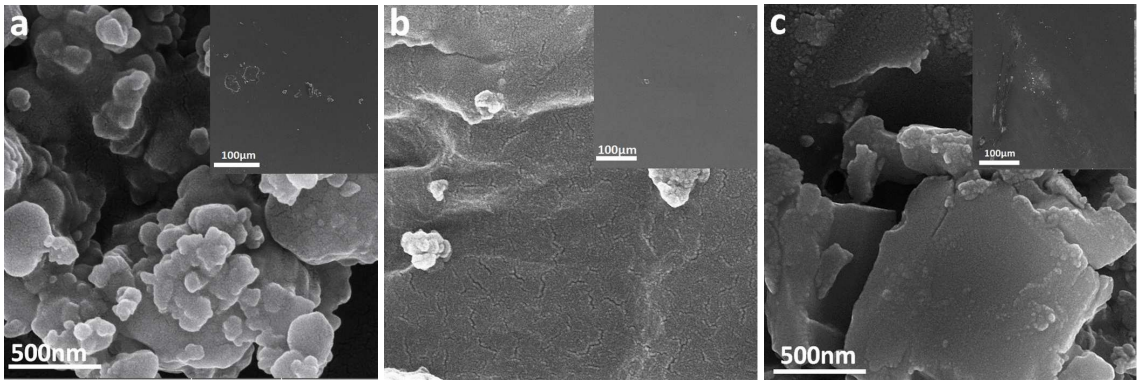

Figure 1. FESEM images of the surface of the prepared coatings in different solutions: a) S1, b) S2 and c) S3

lution. The coating which was prepared via the S2 solution shows a homogeneous distribution of submicron particles. The acidic pH of the solution has led to the linear polymerization in which the monomeric units were linked together to form straight chains. At these conditions relatively small particles were formed. The homogeneity of a coating leads to a uniform self-cleaning property of the coating [13,14]. The fine porosity on the surface of the dried coating leads to the high surface energy of this coating. According to FESEM images, the degree of agglomeration is the lowest in the coating prepared from the S2 solution (having molar ratio of ethanol to TEOS 22:1). It results in better homogeneity of the coating. Indeed, the lower concentration of TEOS is responsible for the film homogeneity. At a relatively low molar ratio of ethanol to TEOS (i.e. the S1 solution), the insufficient volume of ethanol leads to the incomplete TEOS hydrolysis and to the formation of linear chains with organic groups. On the other hand, increasing the molar fraction of ethanol in the solution (i.e. the S3 solution) has led to the increased hydrolysis reaction rate and also to the separation of the sol particles which were formed at the hydrolysis stage. At these conditions, a non-uniform sol structure with big clusters was formed which led to the formation of a weak gel structure with a decreased modulus. As a result, the aggregation of the gel increased. The results of the adhesion test for different samples are given in Table 2. According to the results, it can be declared that the coating had good adhesion to the substrate. Based on the microstructural investigations, among the prepared samples by different solutions, the samples which were coated via the S2 solution were considered for further studies.

Figure 2 shows the result of FTIR analysis of the coating which was calcined at 200 °C. The absorption peaks, detected at 563.14, 786.85 and 925.70 cm^{-1}, correspond to the stretching and bending vibrations of Si–O. Also, the peak with 453.21 cm^{-1} wavenumber is related to the surface vibrations of Si–O binding [15]. The presence of Si–O vibrations at 1060.43 cm^{-1} wavenumber confirms the main structure of SiO_2. Furthermore, some impurity vibrations can be detected in the spectrum with their intensity being lower than that of the main SiO_2. Moreover, the sharp and broad peaks at 1640.79 and 3505.91 cm^{-1} are assigned to the transformation and O–H stretching vibration of water, respectively. Also, the low intensity peaks at 2904.41 and 2998.03 cm^{-1} relate to the symmetric stretching vibration of alkyl groups (i.e. $-CH_2$ and $-CH_3$). It is worth noting that the presence of –OH group is ascribed to the water molecules adsorbed from the air or during the sol-gel process. Apart from the adsorbed water, the synthesized coating is pure SiO_2.

Figure 3 shows the XRD patterns of the coatings calcined at different temperatures. The broad peak observed in the pattern of the calcined coating may be assigned to the low crystallite size and defective structure

Table 2. Adhesion strength of the prepared coatings to the substrate

Applied solution	Adhesion strength [MPa]
S1	1.7
S2	1.7
S3	0.9

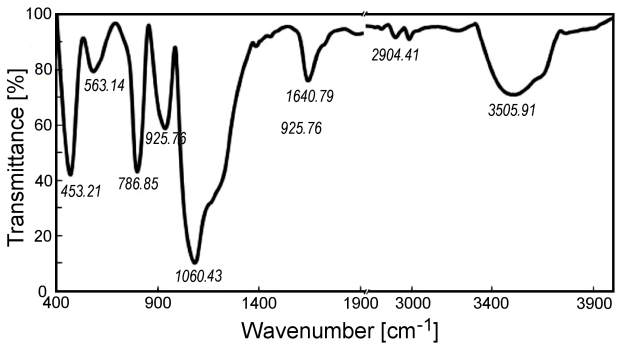

Figure 2. FTIR spectrum of the prepared coating using S2 solution

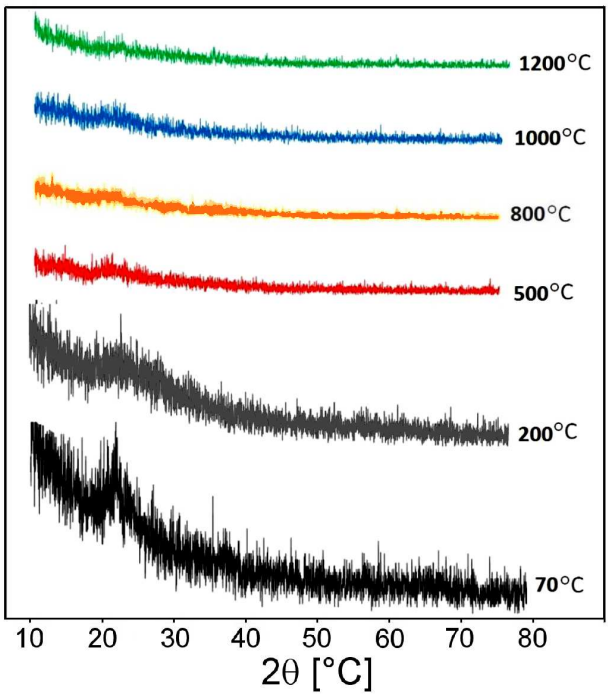

Figure 3. XRD patterns of the coatings prepared using S2 solution calcined at different temperatures

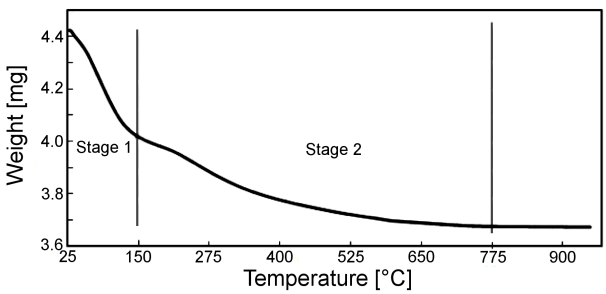

Figure 4. TGA curve of the dried SiO_2 gel

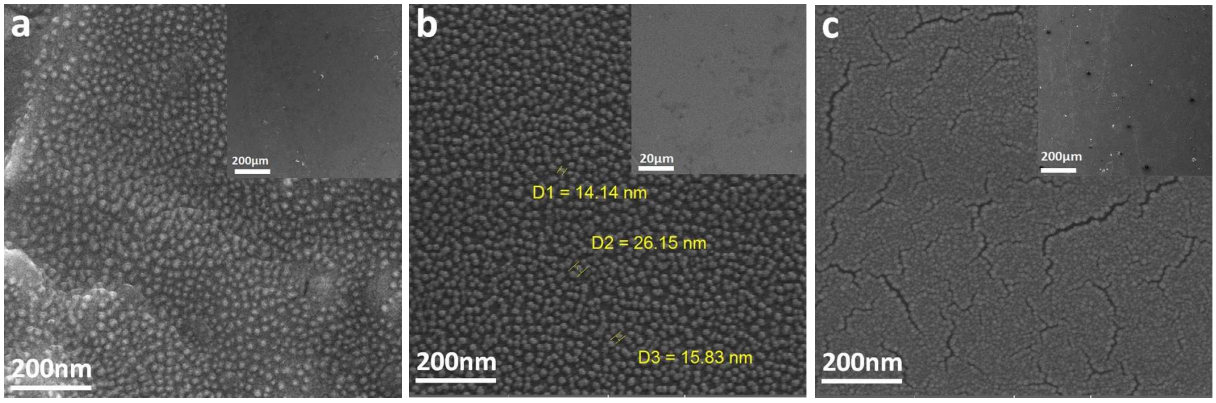

Figure 5. FESEFM micrographs of the samples modified by OTS and ethanol containing solutions with: a) 2, b) 5 and c) 7 vol.% of OTS

of the dried gel. Dubey *et al.* [16] reported that the broad XRD peak confirms the existence of a high volume percent of non-organic particles in the dried gel. The SiO_2 coating has not been crystallized by calcination at temperatures up to 1200 °C, which is in good agreement with the results of other researchers [17].

Figure 4 shows the corresponding TGA curve of the dried SiO_2 gel at room temperature. The curves may be divided into two stages. The first stage from 25 to ~150 °C may be attributed to the gradual evaporation of molecular water and alcohol. The second stage is in the range of 150 to ~775 °C and it is possibly due to the decomposition of the organic compounds. In the second stage, decomposition of the alkoxide-hydroxide and agglomeration of hydroxyl groups occurred on the surface of SiO_2 (Si–OH), respectively. Ek *et al.* [18] reported that the silane groups are stable up to 500 °C, where they start to alkoxidize. Dugas and Chevalier [19] reported that the absorbed water at the surface is mainly evaporated at about 200 °C and just silane groups remain at the surface. At 450 to 500 °C water molecules are formed by the condensation of adjacent silane groups. Above 775 °C, no significant weight loss can be detected, which confirms the decomposition of the silane at lower temperatures. As a result, it can be concluded that the weight loss of the modified sample is due to the decomposition of the alkoxide groups on at SiO_2 surface.

3.2. Modification of the prepared coating

Figure 5 shows the FESEM micrographs of the coatings modified by the dipping in the OTS containing solutions. It can be observed that the coating which was dipped in the 5 vol.% OTS solution shows more homogeneous dispersion of particles than other two samples. On the other hand, in the sample which was dip coated in the 7 vol.% OTS solution, due to the aggregation of particles and decreased viscosity, the volume percent of pores increased and the particles were agglomerated (Fig. 5c). The mean particle size of the coating modified by the 5 vol.% OTS solution was 19 nm. Figure 6 confirms that the thicknesses of the primary and secondary coating were 21 and 43 nm, respectively.

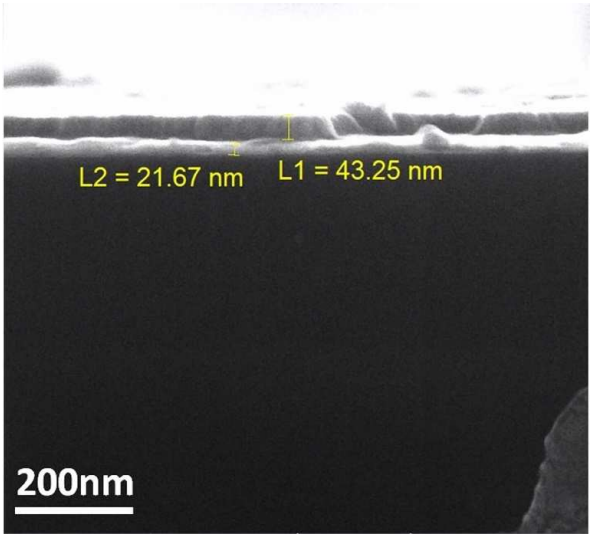

Figure 6. FESEM micrograph of the cross section of SiO_2 coating modified by 5 vol.% OTS solution

Figure 7 shows the AFM micrographs of the modified samples. The AFM results confirm the formation of a nanostructured coating on the surface. The coating modified by 5 vol.% OTS solution was more homogeneous than other samples. No defects like porosity or cracks can be detected on the surface. Furthermore, the surface roughness is 80 nm which is lower than 270 reported by Du *et al.* [12].

3.3. Hydrophobic and electrical properties

Figure 8 shows the images of the water droplets on the glass substrate and on the coatings which were prepared using the S1, S2 and S3 solutions. By applying SiO_2 coating, the contact angle increased. However, the contact angle of the coating prepared via the S2 solution (51°) was the highest among the samples. According to the FESEM and AFM images, the absence of fine porosity and the uniform roughness of this coating have led to the decrease of the surface energy and to the increase of the wetting angle.

Figure 9 shows the image of a water droplet on the coatings which were prepared and modified via the S2 and OTS containing solutions. As it is observed, by

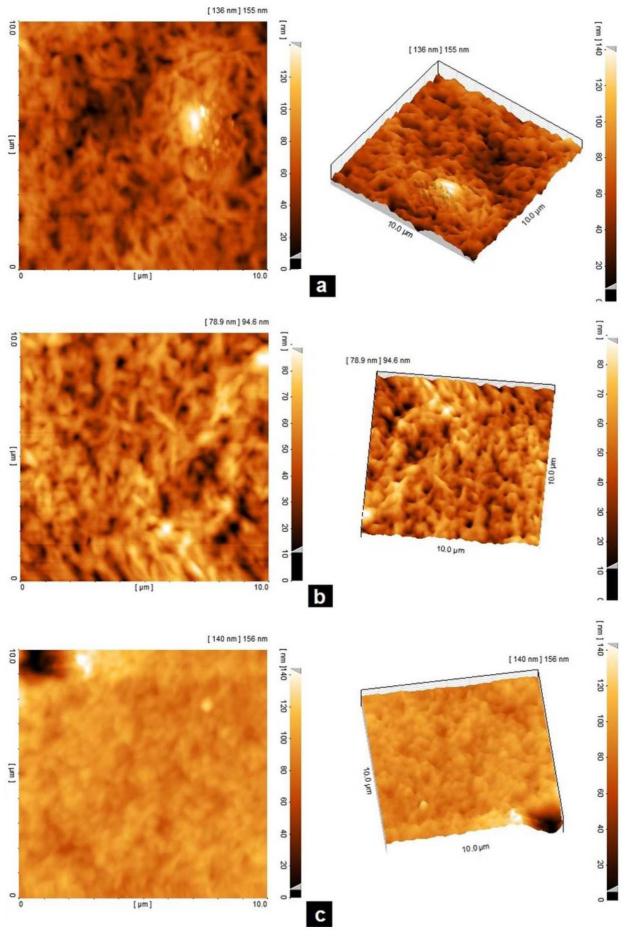

Figure 7. AFM images of the samples modified by: a) 2, b) 5 and c) 7 vol.% of OTS

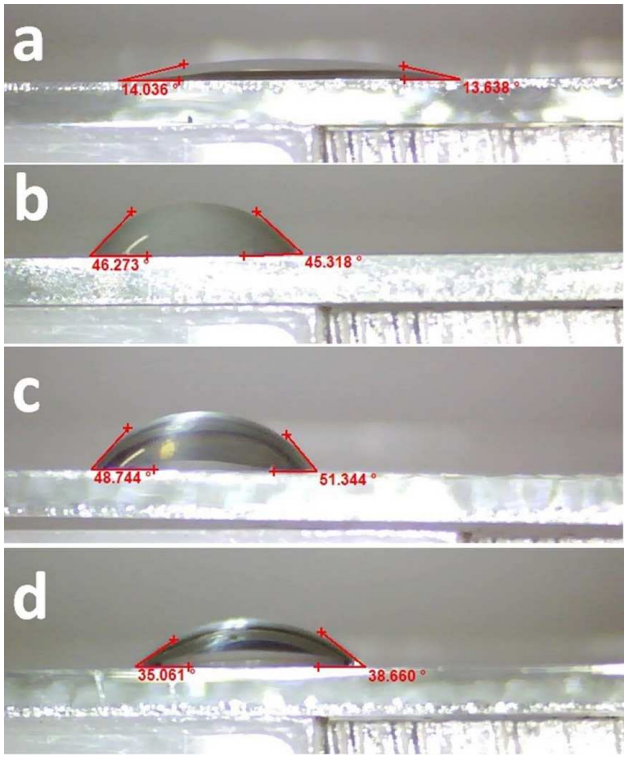

Figure 8. The images of water droplets on: a) glass substrate and the coatings prepared by b) S1, c) S2 and d) S3 solutions

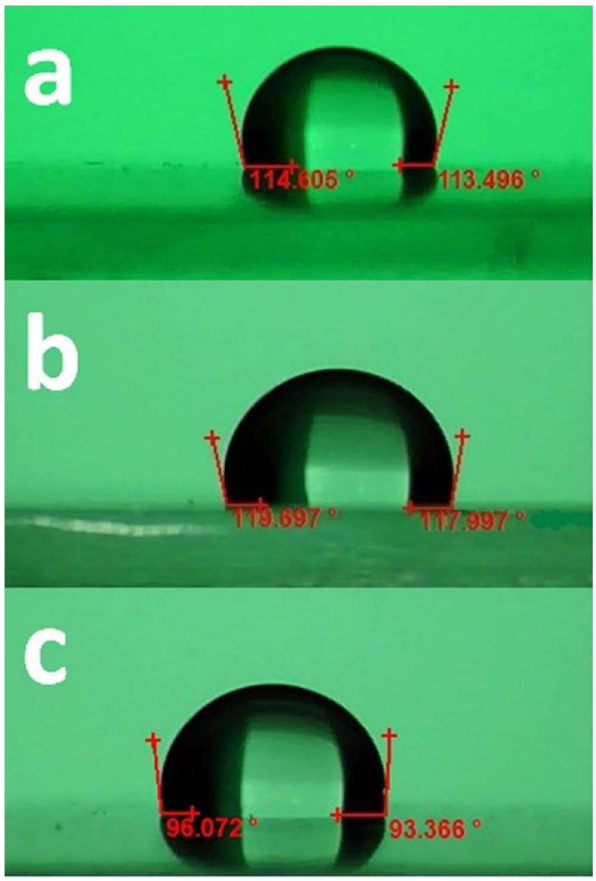

Figure 9. Image of a water droplet on the coatings prepared with S2 solution and modified by: a) 2, b) 5 and c) 7 vol.% of OTS

modifying the coating, the contact angle increased significantly due to the decrease of the surface energy and the presence of functional groups. In other words, according to the Young's equation, by modifying the coating, the surface tension of the glass/water droplet interface increased and the shape of the droplet changed to a hemisphere like the one in Fig. 9.

Figure 10 shows the images of the uncoated and coated outdoor insulators. As observed, the surface of the uncoated insulator has been wetted completely by water droplets. However, the water droplets on the surface of the coated insulator are spherical and the hydrophobic property of the prepared coating is obvious. Figure 11 shows the image of a water droplet on the sur-

Figure 10. The uncoated and coated outdoor insulators

Table 3. Results of leakage current test of the uncoated and coated insulators

Insulator specification	Applied voltage [kV]	Leakage current [μA]	Break down voltage [kV]
Without coating	2.9	8.8	24
	10	32	
Coated with silica nanoparticles, modified by OTS solution	2.9	6.8	24
	10	24.4	

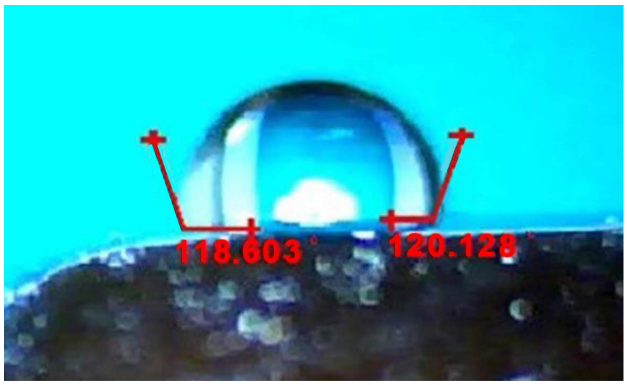

Figure 11. A water droplet on the surface of a coated outdoor insulator after working in an air atmosphere under sunlight for sixty days (contact angle is about 120°)

face of a coated outdoor insulator after working in an air atmosphere under sunlight for sixty days. The measured contact angle was 120°, implying good hydrophobic property of the coating.

Table 3 shows the results of the leakage current tests of the uncoated and coated insulator. It can be declared that by coating the insulator, the leakage current, one of the main factors in the destruction of insulators, decreased for about 25%, which is a remarkable improvement. However, the break down voltage did not change.

IV. Conclusions

In this research, modified silica containing coating was created on the glass and insulator substrates via the sol-gel process. The mean particle size of the silica within the microstructure of the coating was 19 nm. Also, the thickness of the coating was 65 nm after modification by OTS. The topographic investigations by AFM showed a uniform and homogeneous coating without any cracks and porosity with low roughness variations. The results showed that by creating the coating, the contact angle increased from 14 to 51°. However, by modifying the created coating, the contact angle was increased to 119°. Also, the contact angle of the created coating on the outdoor insulator was determined to be 120° after 60 days in atmospheric conditions. It was shown that by creating a silica coating on the surface of the insulator, the leakage current decreased for about 25%.

References

1. K.F. Portella, P. Mengarda, M.S.R. Bragança, O.G.P. Júniora, J.S.S. Melo, D.P. Cerqueira, S.A. Pianaro, M.M. Mazur, "Nanostructured titanium film deposited by pulsed plasma magnetron sputtering (PPMS) on a high voltage ceramic insulator for outdoor use", *Mater. Res.*, **18** [4] (2015) 853–859.
2. D. Zhang, L. Wang, H. Qian, X. Li, "Superhydrophobic surfaces for corrosion protection: a review of recent progresses and future directions", *J. Coat. Technol. Res.*, **13** [1] (2016) 11–29.
3. A. Marsal, F. Ansart, V. Turq, J.P. Bonin, J.M. Sobrino, Y.M. Chen, J. Garcia, "Mechanical properties and tribological behavior of a silica or/and alumina coating prepared by sol-gel route on stainless steel", *Surf. Coat. Technol.*, **237** (2013) 234–240.
4. Z. Wan, T.F. Zhang, H.B.R. Lee, J.H. Yang, W.C. Choi, B. Han, K.H. Kim, S.H. Kwon, "Improved corrosion resistance and mechanical properties of CrN hard coatings with an atomic layer deposited Al_2O_3 interlayer", *ACS Appl. Mater. Interf.*, **7** (2015) 26716–26725.
5. M. Rahman, *Nanomaterials*, Intech Open, Croatia, 2011.
6. R.M. Laine, "Chemical processing of glasses", pp. 16–28 in 34th *Annual International Technical Symposium on Optical and Optoelectronic Applied Science and Engineering*, San Diego, CA, United States, 1990.
7. J. Livage, M. Henry, C. Sanchez, "Sol-gel chemistry of transition metal oxides", *Prog. Solid State Chem.*, **18** (1988) 259–341.
8. C.J. Brinker, G.W. Scherer, *Sol-Gel Science - The Physics and Chemistry of Sol-Gel Processing*, Academic Press, San Diego, CA, United States, 1990.
9. S. Liu, S. Latthe, H. Yang, B. Liu, R. Xing, "Raspberry-like superhydrophobic silica coatings with self-cleaning properties", *Ceram. Int.*, **41** (2015) 11719–11726.
10. I. Ramalla, R. Gupta, K. Bansal, "Effect on superhydrophobic surfaces on electrical porcelain insulator, improved technique at polluted areas for longer life and reliability", *Int. J. Eng. Technol.*, **4** (2015) 509–519.
11. M. Pantoja, J. Abenojar, M.A. Martinez, "Influence of the type of solvent on the development of superhydrophobicity from silane-based solution containing nanoparticles", *Appl. Surf. Sci.*, **397** (2017) 87–94.
12. W. Dou, P. Wang, D. Zhang, J. Yu, "An efficient way to prepare hydrophobic anti reflective SiO_2 film by sol-gel method", *Mater. Lett.*, **167** (2016) 69–72.
13. R. Zhang, L. Gao, "Preparation of nanosized titania by hydrolysis of alkoxide titanium in micelles", *Mater. Res. Bull.*, **37** (2002) 1659–1666.
14. R. Blossey, "Self-cleaning surfaces-virtual realities", *Nat. Mater.*, **2** (2003) 301–306.
15. Q. Guo, D. Huang, X. Kou, W. Cao, L. Li, L. Ge, J. Li, "Synthesis of disperse amorphous SiO_2 nanoparticles via sol-gel process", *Ceram. Int.*, **43** (2017) 192–196.
16. R.S. Dubey, Y. Rajesh, M.A. More, "Synthesis and characterization of SiO_2 nanoparticles via sol-gel method for industrial applications", *Mater. Today Proceed.*, **2** (2015) 3575–3579.

17. M.G. Garnica-Romo, J.M. Yanez-Limon, M. Villican, J.F. Perez-Robles, R. Zamorano-Ulloa, J. Gonzalez-Hernandez, "Structural evolution of sol-gel SiO_2 heated glasses containing silver particles", *J. Phys. Chem. Solids*, **65** (2004) 1045–1052.
18. S. Ek, A. Root, M. Peussa, L. Niiniso, "Determination of the hydroxyl group content in silica by thermogravimetry and a comparison with 1H MAS NMR results", *Thermochim. Acta*, **379** (2001) 201–212.
19. V. Dugas, Y. Chevalier, "Surface hydroxylation and silane grafting on fumed and thermal silica", *J. Colloid Interf. Sci.*, **264** (2003) 354–361.